Soil & Tillage Research 255 (2026) 106802

Contents lists available at ScienceDirect

Soil & Tillage Research

journal homepage: www.elsevier.com/locate/still

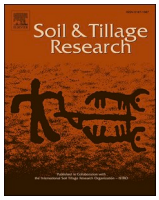

Root processes counteract the suppression of nitrogen-induced priming effects by enhancing microbial activity and catabolism in greenhouse vegetable production systems

Jinshan Lian [a,b,c], Sébastien Massart [b], Guihua Li [a,c,*], Jianfeng Zhang [a,c,d,*]

[a] State Key Laboratory of Efficient Utilization of Arid and Semi-arid Arable Land in Northern China, Institute of Agricultural Resources and Regional Planning, Chinese Academy of Agricultural Sciences, Beijing 100081, China
[b] Laboratory of Integrated and Urban Phytopathology, TERRA, Gembloux Agro-Bio Tech, University of Liège, Passage des déportés 2, Gembloux 5030, Belgium
[c] National Center of Technology Innovation for Comprehensive Utilization of Saline-Alkali Land. Innovation for Comprehensive Utilization of Saline-Alkali Land, Shandong 257000, China
[d] Institute of Special Animal and Plant Sciences, Chinese Academy of Agricultural Sciences, Changchun 130112, China

ARTICLE INFO

Keywords:
Nitrogen fertilization
Priming effect
Rhizosphere processes
Microbial carbon use efficiency
^{13}C-labeling
Greenhouse vegetable production

ABSTRACT

Nitrogen (N) fertilization regulates soil organic carbon (SOC) decomposition by altering the priming effect (PE) and root activities, affecting subsequently soil carbon sequestration and crop productivity. However, the effects of long-term N fertilization on the direction and magnitude of SOC and underlying mechanisms priming in the rhizosphere compared with bulk soils remain unclear. In this study, paired rhizosphere and bulk soil samples were collected from a 15-year greenhouse tomato production system under four chemical N fertilizer treatments: 0 (N0), 102 (N1), 327 (N2), and 552 (N3) kg N ha^{-1} yr^{-1}, in addition to uniform manure and straw amendment at 123 kg N ha^{-1} yr^{-1}. These samples were incubated for 49 days with or without the addition of ^{13}C-labeled glucose, and the incorporation of glucose-derived ^{13}C into CO_2 and phospholipid fatty acids (PLFAs) was monitored to elucidate the mechanisms underlying the PE. The results showed a significant interaction between N fertilization and soil niche. The relative PE was significantly higher under the N0 treatment (1.82–2.02 %) compared with the strongly negative values observed under N1–N3 treatments (-0.81 % to -10.18 %) in both rhizosphere and bulk soils, indicating that increased N availability suppressed SOC decomposition. However, rhizosphere soils exhibited significantly weaker negative PE (-2.66 %) than bulk soils (-4.36 %), primarily due to lower dissolved organic nitrogen (DON) levels and higher microbial abundance and activity, suggesting that rhizosphere processes partially counteracted the suppressive effect of N fertilization. A reduction in relative PE correlated with increases in dissolved organic nitrogen (DON), glucose-derived microbial biomass carbon (^{13}MBC), and microbial carbon use efficiency (CUE). Overall, long-term N fertilization suppressed SOC priming by enhancing soil N availability and microbial C assimilation capacity. However, root-mediated microbial legacy effects in the rhizosphere counteracted this suppression, highlighting the importance of N–soil niche interactions in regulating SOC turnover. These findings offer novel insights into soil carbon cycling dynamics and have implications for targeted soil carbon sequestration strategies in intensive greenhouse agriculture.

1. Introduction

Nitrogen (N) fertilization is essential in crop production in agricultural ecosystems. However, long-term and intensive N fertilization, along with other agricultural practices, significantly alters soil properties, including soil organic carbon (SOC) dynamics (Schmidt et al., 2011; Xu et al., 2022). Numerous studies have shown that long-term N input substantially modifies the physicochemical and biological characteristics of soil in greenhouse vegetable production (GVP) systems (Kianpoor Kalkhajeh et al., 2021; Wang et al., 2024c; Zhang et al., 2023). These alterations likely influence SOC decomposition through complex interactions (Liang et al., 2019). Therefore, elucidating the mechanisms

* Corresponding authors at: State Key Laboratory of Efficient Utilization of Arid and Semi-arid Arable Land in Northern China, Institute of Agricultural Resources and Regional Planning, Chinese Academy of Agricultural Sciences, Beijing 100081, China.
E-mail addresses: liguihua@caas.cn (G. Li), zhangjianfeng@caas.cn (J. Zhang).

https://doi.org/10.1016/j.still.2025.106802
Received 2 April 2025; Received in revised form 7 August 2025; Accepted 9 August 2025
Available online 16 August 2025

underlying SOC turnover under long-term N fertilizer application is crucial for accurately assessing the impact of N management on soil carbon sequestration potential and sustainability in GVP systems.

The content of SOC largely depends on the balance between inputs from external organic resources and outputs from microbial decomposition. However, newly added organic carbon could either stimulate or inhibit the microbial decomposition of native SOC—a phenomenon known as the positive or negative priming effect (PE), which can vary from -50 % to + 380 % across different ecosystems (Kuzyakov et al., 2000; Shahbaz et al., 2017). Researchers have extensively investigated the key drivers of this variability, including substrate availability as well as soil physicochemical and microbial properties (Li et al., 2023; Zhou et al., 2022). Numerous studies have reported that both the direction and intensity of PE are associated with soil nutrient accessibility (Feng and Zhu, 2021; Feng et al., 2021; Zhang et al., 2024). For example, soil N availability directly affects the PE by altering microbial nutrient acquisition strategies (Qin et al., 2024), and indirectly by modifying soil physicochemical properties (Aye et al., 2018; Lenka et al., 2019).

Despite extensive research using both field and laboratory experiments, the response of the PE to N availability remains inconsistent and sometimes contradictory, with some studies reporting an increase (Meyer et al., 2018; Zheng et al., 2022), others a decrease (Ma et al., 2024; Su and Shangguan, 2023) and some finding no significant change (Fang et al., 2018). To explain these contrasting findings, two contradictory theories have been proposed. The first, the stoichiometric decomposition theory, suggests that microbial decomposition of native SOC reaches its maximum rate when the supply of soil substrates (carbon or nutrients) meets microbial metabolic demands (Rocci et al., 2024). The second, the microbial N mining theory, hypothesizes that PE is lower in N-rich soils than in N-deficient soils, because microbes in nutrient-rich environments have less need to decompose recalcitrant SOC for N acquisition (Craine et al., 2007). These inconsistent PE responses highlight the need for further research to clarify their complex relationship with soil N availability.

The effects of N fertilization on the priming effect (PE) are largely mediated by changes in soil microbial community composition and function, including shifts in carbon use efficiency and nutrient acquisition strategies (Domeignoz-Horta et al., 2020). Specific microbial taxa contribute to this process by producing extracellular enzymes that degrade complex organic matter into assimilable forms (Wu et al., 2022). Long-term chemical N fertilization fundamentally alters microbial metabolic processes and assimilation efficiency by modifying microbial activity and community composition, which in turn impacts SOC priming dynamics (Geisseler and Scow, 2014; Dai et al., 2018; Jia et al., 2020). Xu et al. (2022), (2024) further highlighted that in Chinese vegetable soils, the priming effect is primarily driven by microbial traits, including microbial richness and carbon use efficiency, which directly modulate SOC stability. This finding underscores the pivotal role of microbial community characteristics in determining the magnitude and direction of PE in response to N fertilization.

Microbial carbon use efficiency (CUE) is defined as the proportion of assimilated carbon allocated to biomass production relative to that lost through respiration, serving as an essential proxy (Sinsabaugh et al., 2013). According to the stoichiometric homeostasis theory, microbial CUE decreases under N-deficient conditions because more carbon is diverted toward N acquisition (Manzoni et al., 2012). Conversely, increased N inputs from N fertilizer application lower the soil carbon-to-nitrogen (C:N), enhancing microbial growth and CUE while simultaneously reducing the PE (Finn et al., 2015). On the other hand, N-rich soils may suppress microbial CUE by favoring fast-growing microbes that exhibit higher energy demands (Luo et al., 2020). However, the mechanistic understanding of how long-term N fertilization regulates microbial CUE and influences SOC priming intensity remains incomplete, warranting further investigation.

The rhizosphere—a distinct soil volume influenced by root-mediated processes—plays a crucial role in controlling SOC turnover and nutrient cycling (Kuzyakov and Blagodatskaya, 2015). Characterized by unique physical, chemical and biological processes, the rhizosphere exhibits greater nutrient availability and elevated microbial activity compared with bulk soils (Kuzyakov and Xu, 2013; Liu et al., 2022; Wang and Kuzyakov, 2024). Rhizodeposition, which accounts for approximately 10–50 % of the carbon assimilated by plants through photosynthesis, plays a crucial role in shaping soil carbon dynamics and influencing carbon sequestration and climate feedbacks (Zang et al., 2017; Pausch and Kuzyakov, 2018). Generally, studies have reported that rhizosphere soils accelerate SOC decomposition via the PE, largely driven by microbial responses to C inputs such as root exudates, which stimulate microbial activity and soil enzyme production (Chen et al., 2021). In contrast, high microbial abundance and activity in rhizosphere soils are favorable for SOC sequestration through microbial assimilation and turnover of root-derived C inputs (Wang et al., 2024b; Villarino et al., 2025). However, the effects of long-term N fertilization on SOC priming in response to exogenous C inputs in the rhizosphere relative to bulk soils in the GVP agroecosystem remain unclear.

In this context, the long-term study assessing the effects of chemical N fertilization on yield and SOC sequestration in the GVP system (Lian et al., 2024) provides a valuable framework for further exploring SOC priming dynamics. Therefore, the objectives of this study were to (i) investigate the effects of long-term N fertilization on SOC priming in both rhizosphere and bulk soils in GVP system, and (ii) elucidate the underlying mechanisms and driving factors for SOC priming. We hypothesized that (i) long-term N fertilization would decrease the PE due to increased soil N availability; (ii) the rhizosphere soils would exhibit a more pronounced PE compared with bulk soils, primarily attributed to enhanced microbial abundance and activity; (iii) the effect of N fertilization on PE may differ between rhizosphere and bulk soils due to their contrasting microbial and biochemical environments.

2. Materials and methods

2.1. Soil sampling and glucose preparation

The experiment was conducted based on a long-term field trial established in a greenhouse vegetable production system located in Hebei, China (115°17'53"E, 37°47'55"N) starting in 2008, with an annual rotation of cucumbers and tomatoes. The study area has a semi-humid continental monsoon climate, characterized by an average annual temperature of 11.5 °C and annual precipitation of 540 mm. The soil type is classified as a Fluvo-aquic soil with a loamy texture. The initial physicochemical properties of the soil were as follows: pH 8.1 (soil-water ratio 1:2.5, 25 ℃), soil organic carbon (SOC) content of 5.0 g kg^{-1}, total nitrogen (TN) content of 1.55 g kg^{-1}, total phosphorus (TP) content of 1.0 g kg^{-1}, total potassium (TK) content of 15.2 g kg^{-1}, Olsen-P (AP) content of 82.9 mg kg^{-1}, available potassium (AK) content of 60.0 mg kg^{-1}, nitrate nitrogen (NO_3^-) content of 5.5 mg kg^{-1} and ammonium nitrogen (NH_4^+) content of 19.4 mg kg^{-1}. Electrical conductivity (EC) was 307.4 μS cm^{-1} at a water-soil ratio of 5:1 at 25 ℃. The soil bulk density was 1.35 g cm^{-3}. The experiment was carried out with a randomized block design with four treatments and three replicates per treatment. Each plot measured 10.8 m^2 (1.8 m width × 6.0 m length).

Four N fertilizer application rates were selected for tomato cultivation: no chemical nitrogen (N0), 102 kg chemical N ha^{-1} yr^{-1}(N1), 327 kg chemical N ha^{-1} yr^{-1}(N2), and 552 kg chemical N ha^{-1} yr^{-1}(N3), all applied as urea. The phosphorus (P_2O_5) application remained constant at 0 kg ha^{-1} yr^{-1}, while potassium (K_2O) was applied at a rate of 210.6 kg ha^{-1} yr^{-1} for all treatments. Additionally, chicken manure was applied annually at a rate of 1560 kg ha^{-1} (on a dry weight basis), containing 23 kg N ha^{-1}, 51 kg P_2O_5 ha^{-1}, and 36 kg K_2O ha^{-1}. Wheat straw also was applied annually at a rate of 14,599 kg ha^{-1} (dry weight basis), containing 100 kg N ha^{-1}, 24 kg P_2O_5 ha^{-1}, and 203 kg K_2O ha^{-1}. As a result, the total N input for each treatment was 123, 225, 450, and 675 kg N ha^{-1} yr^{-1}, respectively. Urea and potassium fertilizers were

applied in three stages: pre-planting (as a base fertilizer), mid-growth (approximately 30–40 days after transplanting), and pre-flowering (approximately 60–80 days after transplanting). The remaining fertilizers, including potassium (K_2O), chicken manure, and wheat straw, were incorporated once as a base fertilizer.

On January 20, 2023, 150 days after the transplanting of tomato seedlings (pulling period), soil samples were collected from 0–20 cm layer. Rhizosphere soil samples were collected by gently shaking the roots to remove loosely adhered soil. The soil tightly adhered to roots was defined as rhizosphere soil (Edwards et al., 2015; Li et al., 2020). Bulk (non-rhizosphere) soils were sampled from adjacent unplanted areas within the same treatment plots, at the same depth as the rhizosphere soil, to ensure consistency across treatments (Fig. S1). Three subsamples were collected from each plot and thoroughly mixed to form one composite sample per plot. All soil samples were transported to the laboratory, sieved (<2 mm), and divided into two parts. One subsamples of rhizosphere and bulk soils were stored at 4 ℃ for the analysis of enzyme activity, microbial biomass, and the glucose addition experiment. The remaining samples were air-dried for the determination of soil physical and chemical properties.

We selected glucose because it is a major component of root exudates and can be rapidly utilized by most microbes (Gunina and Kuzyakov, 2015). The ^{13}C-glucose used corresponded to a 20:1 mixture of ^{12}C-glucose and ^{13}C-glucose (99 % atom), and its isotopic abundance was 5409 ‰ (Gunina and Kuzyakov, 2015).

2.2. Incubation experiment

The soil samples stored at 4 ℃ were pre-incubated for one week at 25 ℃ and 60 % water-holding capacity (WHC) to activate microbial activity. Following pre-incubation, soil samples were amended with ^{13}C-glucose at 2 % of the initial SOC content for each treatment (Table S1). Glucose was used to simulate labile C input as it is a major component of root exudates and products of litter decomposition (Gunina and Kuzyakov, 2015). This application rate was selected based on previous studies, which showed that the added carbon amounted to 53–100 % of the initial microbial biomass carbon (Whitaker et al., 2014). This proportion was sufficient to stimulate microbial activity and respiration without significantly promoting microbial growth (Blagodatskaya and Kuzyakov, 2008). The treated soil samples (equivalent to 50 g oven-dried soil) were then transferred to 250 mL air-tight Mason jars and incubated at 25 ℃ and 60 % WHC for 49 days. Four soil-free Mason jars were included as blanks to account for background CO_2 emissions. During the incubation period, soil moisture was maintained at 60 % WHC by periodically adding sterile deionized water. CO_2 gas samples were collected using a 20 mL syringe on days 1, 3, 5, 7, 14, 23, 34, and 49 of incubation. At each sampling time, the jars were ventilated with CO_2-free air for 20 min. CO_2 concentration and its ^{13}C isotopic signature were measured using a 6890 N gas chromatograph (Agilent Technologies, Palo Alto, CA) and an isotope ratio mass spectrometer (IRMS) coupled with a Gas Bench (Thermo Finnigan, San Jose, CA).

The CO_2 emitted from the glucose-amended treatments was separated into SOC-derived and glucose-derived components using a two-pool isotopic mixing model:

$$CO_{2\ \mathrm{Glu-derived}} = CO_{2\ \mathrm{total}} \times \frac{\delta^{13}CO_{2\ \mathrm{total}} - \delta^{13}CO_{2\ \mathrm{control}}}{\delta^{13}CO_{2\ \mathrm{Glu}} - \delta^{13}CO_{2\ \mathrm{control}}} \quad (1)$$

$$CO_{2\ \mathrm{SOC-derived}} = CO_{2\ \mathrm{total}} - CO_{2\ \mathrm{Glu-derived}} \quad (2)$$

where $CO_{2\ \mathrm{Glu\text{-}derived}}$, $CO_{2\ \mathrm{SOC\text{-}derived}}$, and $CO_{2\ \mathrm{total}}$ refer to the glucose-derived CO_2-C, SOC-derived CO_2-C, and total CO_2-C emitted from glucose-amended soils, respectively. $\delta^{13}CO_{2\ Glu}$, $\delta^{13}CO_{2\ control}$, and $\delta^{13}CO_{2\ total}$ represent the $\delta^{13}C$ (‰) values of the CO_2 evolved from pure glucose, glucose-unamended soil, and the corresponding glucose-amended soil respectively.

The priming effect (PE) was calculated as follows:

$$\mathrm{PE} = \text{amended } CO_{2\ \mathrm{SOC-derived}} - \text{unamended } CO_{2\ \mathrm{SOC-derived}} \quad (3)$$

$$\text{Relative PE}\ (\%) = \frac{\text{amended } CO_{2\ \mathrm{SOC-derived}} - \text{unamended } CO_{2\ \mathrm{SOC-derived}}}{\text{unamended } CO_{2\ \mathrm{SOC-derived}}} \quad (4)$$

where amended $CO_{2\ \mathrm{SOC\text{-}derived}}$ and unamended $CO_{2\ \mathrm{SOC\text{-}derived}}$ represent the cumulative CO_2 emissions (mg C kg^{-1} soil) derived from SOC in the glucose-amended and corresponding glucose-unamended treatments, respectively.

2.3. Soil properties analysis

Soil pH was measured using a pH meter with a soil to water ratio of 1:2.5 (w/v). Soil organic carbon (SOC) content was determined using the potassium dichromate oxidation method. Total nitrogen (TN) was determined by the Kjeldahl digestion method (Bremner and Mulvaney, 1983). Olsen phosphorus (Olsen-P) and available potassium (AK) were measured using Olsen method (Olsen and Sommers, 1983) and flame photometry, respectively. Soil ammonium-nitrogen (NH_4^+–N) and nitrate-nitrogen (NO_3^-–N) were extracted with 2 M KCl and measured by a continuous flow analyser (Kachurina et al., 2000) (Autoanalyzer 3, Bran and Luebbe, Germany). Mineral nitrogen (MN) content was calculated as the sum of NH_4^+–N and NO_3^-–N.

Microbial biomass carbon (MBC) was determined using chloroform fumigation-extraction method (Wu et al., 1990). Briefly, 10.0 g of soil sample was fumigated using a desiccator with ethanol-free chloroform ($CHCl_3$) and 2 M NaOH for 24 h in the dark at 25 °C, while corresponding 10.0 g soil sample was placed in another desiccator without $CHCl_3$ under the same condition. All soil samples were immediately extracted with 0.05 M K_2SO_4 for 30 min at 180 rpm. Total organic carbon (TOC) in the K_2SO_4 extracts was analyzed using a total organic carbon analyzer (Multi C/N 3100, Germany). The difference in organic C concentrations between fumigated and non-fumigated extracts was calculated as MBC using a conversion factor ($K_{EC} = 0.45$). The extracts from non-fumigated samples were also used to measure dissolved organic carbon (DOC) and dissolved organic nitrogen (DON). The remaining K_2SO_4 extracts were freeze-dried to determine the $\delta^{13}C$ values of MBC using an isotope ratio mass spectrometer.

The $\delta^{13}C$ value of MBC (δ^{13}MBC) was calculated using the following equation:

$$\delta^{13}\mathrm{MBC} = \frac{\delta^{13}C_{\mathrm{fumi}} \times C_{\mathrm{fumi}} - \delta^{13}C_{\mathrm{unfumi}} \times C_{\mathrm{unfumi}}}{C_{\mathrm{fumi}} - C_{\mathrm{unfumi}}} \quad (5)$$

where $\delta^{13}C_{fumi}$ and $\delta^{13}C_{unfumi}$ represent the $\delta^{13}C$ values of the extracts from the fumigated and corresponding non-fumigated soils, respectively, and C_{fumi} and C_{unfumi} represent the DOC contents (mg C kg^{-1} soil) of the extracts from the fumigated and non-fumigated soils, respectively.

The amount of glucose-derived MBC (^{13}MBC) in the glucose-amended soils was calculated as follows:

$$\mathrm{Glu-derived\ MBC}\ (^{13}\mathrm{MBC}) = \mathrm{MBC_{total}} \times \frac{\delta^{13}C_{\mathrm{MBC}} - \delta^{13}C_{\mathrm{UN\ MBC}}}{\delta^{13}C_{\mathrm{glu}} - \delta^{13}C_{\mathrm{UN\ MBC}}} \quad (6)$$

where MBC_{total} is the content of MBC in the glucose-amended soil, and $\delta^{13}C_{MBC}$ and $\delta^{13}C_{UN\ MBC}$ are the $\delta^{13}C$ values of MBC from the glucose-amended and corresponding glucose-unamended soils, respectively. $\delta^{13}C_{glu}$ is the actual $\delta^{13}C$ value of the glucose substrate.

The microbial carbon use efficiency (CUE) was calculated as the ratio of glucose-derived MBC to total glucose-C uptake (sum of glucose-derived MBC and glucose-derived CO_2).

$$CUE = \frac{MBC_{glucose-derived}}{MBC_{glucose-derived} + CO_{2glucose-derived}} \quad (7)$$

2.4. Phospholipid fatty acid and enzyme activity analysis

At the end of incubation (49 days), soil samples were collected for phospholipid fatty acid (PLFA) and enzyme activity analysis. The PLFAs were measured to determine microbial community composition (Hicks et al., 2019). Briefly, 3.0 g of freeze-dried soil sample was added to 20 mL extraction reagent (chloroform: methanol: citric acid = 1:2:0.8 v/v/v) to extract the total lipids of microbes, and then separated by a 3 mL silica gel column to extract PLFAs, which were subjected to alkaline methylation. PLFA concentrations were determined using the PLFA module of the MIDI Sherlock Microbial Identification System platform of an Agilent 6890 N gas chromatograph (Palo Alto, CA, USA) with Agilent 19091B-102 (25 m × 200 μm × 0.33 μm) column. The internal standard of methyl nonadecanoate (19:0) was used to quantify the phospholipid concentrations. The ^{13}C concentration of each PLFA was analyzed using a Trace GC Ultra gas chromatograph (GC) with a combustion column attached via GC Combustion III to a Delta V Advantage isotope ratio mass spectrometer (Varian Associates Inc., Walnut Creek, CA, USA). The following PLFAs were used as biomarkers for different microbial functional groups: nonspecific bacteria, gram-positive bacteria (G^+), gram-negative bacteria (G^-), and fungi (F), as previously described by Yang et al. (2022). Specifically, G^+ were indicated by 15:0iso, 15:0anteiso, 15:1isoω6c, 16:0iso, 17:0iso, and 17:0anteiso (nmol g^{-1} soil); G^- were represented by 16:1ω7c, 16:1ω9c, 17:1ω8c, 18:1ω5c, 18:1ω7c, 21:1ω3c, 17:0cyclow7c, and 19:0cyclow7c (nmol g^{-1} soil); Fungal biomass was assessed using 18:1ω9c and 18:2ω6c (nmol g^{-1} soil). Total bacterial biomass was calculated as the sum of G^+, G^- and non-specific bacteria, including 14:0, 15:0, 15:0DMA, 16:0, 17:0, 18:0, and 20:0 (nmol g^{-1} soil).

The activities of C-acquiring enzyme (β-1,4-glucosidase, BG; cellobiohydrolase; CBH) and N-acquiring enzyme (leucine aminopeptidase, LAP; β-N-acetylglucosaminidase, NAG) were measured with fluorometric techniques. Briefly, 1.0 g of fresh soil was transferred into a 100 mL sodium acetate buffer (pH 7.0) and shaken for 1–2 min. Subsequently, 200 μL aliquots of soil suspension were transferred into 96-well black microplates containing 50 μL of substrate, buffer, or standard solutions, and incubated for 4 h at a constant temperature of 25 ℃. The activities of the above-mentioned enzymes were determined using a multifunctional microplate reader (Synergy H1M, BioTek Instruments, Inc., Winooski, VT, USA) at excitation and emission wavelengths of 365 nm and 450 nm, respectively.

2.5. Statistical analyses

The normality of the data was tested using the Shapiro-Wilk test ($P > 0.05$) in IBM SPSS Statistics 21.0 (SPSS Inc., Chicago, IL, USA). Two-way ANOVA followed by Duncan's significance test was performed to evaluate the effects of rhizosphere, N fertilization, and their interaction on (i) soil properties (SOC, TN, DOC, DON, DOC:DON ratio); (ii) microbial properties (MBC, PLFAs); (iii) microbial assimilation capacity (the proportion of glucose-derived C incorporated into MBC and PLFAs, microbial CUE); (iv) enzyme activities (LAP, NAG, CBH, BG); and (v) cumulative CO_2 emission, PE and relative PE. Due to the strong collinearity among different factors, partial correlations analysis was carried out to assess the relationship between the relative PE and various factors. The relative importance and significance ($P < 0.05$) of the factors influencing the relative PE were evaluated using the Random Forest model in the R statistical software v.4.3.2 with "randomForest" and "rfPermute" packages. Partial least squares path modeling (PLS-PM) was further conducted to identify the specific effect pathways of relative PE using the R with "plspm" package.

3. Results

3.1. CO_2 emission and priming effect

CO_2 emission and PE were strongly influenced by fertilization, soil niches (bulk vs. rhizosphere soil), and their interaction (Fig. 1). In the absence of glucose, CO_2 emissions in the bulk soils from N2 and N3 treatments significantly decreased by 5 %–7 % compared with N1 treatment ($P < 0.05$; Eqs. (1) and (2)), whereas no significant differences were observed among N fertilizer treatments in the rhizosphere soils (Fig. 1a). When glucose was added, SOC-derived CO_2 emission significantly decreased in both bulk and rhizosphere soils under N fertilization (N1, N2 and N3 treatments) compared with N0 treatment, with primed CO_2 decreasing by 3.1–3.6 times in bulk soils and 1.4–6.0 times in rhizosphere soils (Fig. 1b; Eq. (3)). The relative intensity of PE varied considerably across N fertilizer treatments, with significantly higher values in the N0 treatment compared with N fertilizer treatments in both bulk and rhizosphere soils (Fig. 1c; Eq. (4)). The lowest PE intensity occurred in the N2 treatment (–10 %) in the bulk soils, although no significantly differences were found among the N fertilizer treatments in the rhizosphere soils (Fig. 1c). On average across all N fertilizer treatments, rhizosphere soils exhibited lower PE and relative PE (–8.6 mg kg^{-1} soil and –2.7 %, respectively) than bulk soils (–12.5 mg kg^{-1} soil and –4.4 %, respectively; Fig. 1 bc).

3.2. Changes in soil properties

Long-term N fertilizer application significantly altered soil physical and chemical properties (Table 1; Fig. 2). Compared with N0 treatment, soil pH decreased by 0.07 and 0.34 under N3 treatment in bulk and rhizosphere soils, respectively ($P < 0.05$). SOC content increased by 8.6–11.6 % and 20.0–35.1 % under N2 and N3 treatments compared with N0 treatment in bulk and rhizosphere soils, respectively ($P < 0.05$). In the rhizosphere soils, TN content increased by 15.3–24.3 % under N2 and N3 treatments compared with N0 treatment ($P < 0.05$).

Long-term N fertilizer application also significantly promoted N availability, as indicated by increased DON content and decreased DOC: DON ratio (Fig. 2; $P < 0.05$). Specifically, DON content increased by 1.0–1.5 times in bulk soils and by 1.7–5.3 times in rhizosphere soils under the N2 and N3 treatments compared with N0 treatment ($P < 0.05$). Additionally, the DOC:DON ratio decreased by 6.4–60.1 % in bulk soils and by 45.6–83.0 % in rhizosphere soils under the N1–N3 treatments relative to N0 treatment ($P < 0.05$). Across all treatments, DON content was significantly higher in bulk soils (16.7–42.0 mg kg^{-1}) than in rhizosphere soils (4.4–27.9 mg kg^{-1}; $P < 0.05$). In contrast the N3 treatment significantly increased DOC content by 5.5 %–8.5 % compared with the N0, N1 and N2 treatments in rhizosphere soils, whereas no significant changes were observed in bulk soils.

3.3. Changes in soil microbial properties

Microbial PLFAs varied across N fertilizer treatments, with significantly higher levels in N3 treatment, followed by the N2 and N1 treatments, and lowest in N0 treatment in the rhizosphere soils (Fig. S2). The proportion of glucose-derived C incorporated into PLFAs was significantly affected by fertilization, rhizosphere effect, and their interaction (Fig. 3). On average, microbial assimilation capacity, including ^{13}PLFA, ^{13}Bacteria, ^{13}Fungal, $^{13}G^-$, and $^{13}G^+$ were significantly higher in rhizosphere soils than in bulk soils (Fig. 3a). Specifically, rhizosphere soils exhibited increase in ^{13}PLFA by 34.0 %, ^{13}bacteria by 35.4 % and ^{13}fungi by 22.5 % compared with bulk soils across N fertilizer treatment, respectively ($P < 0.05$).

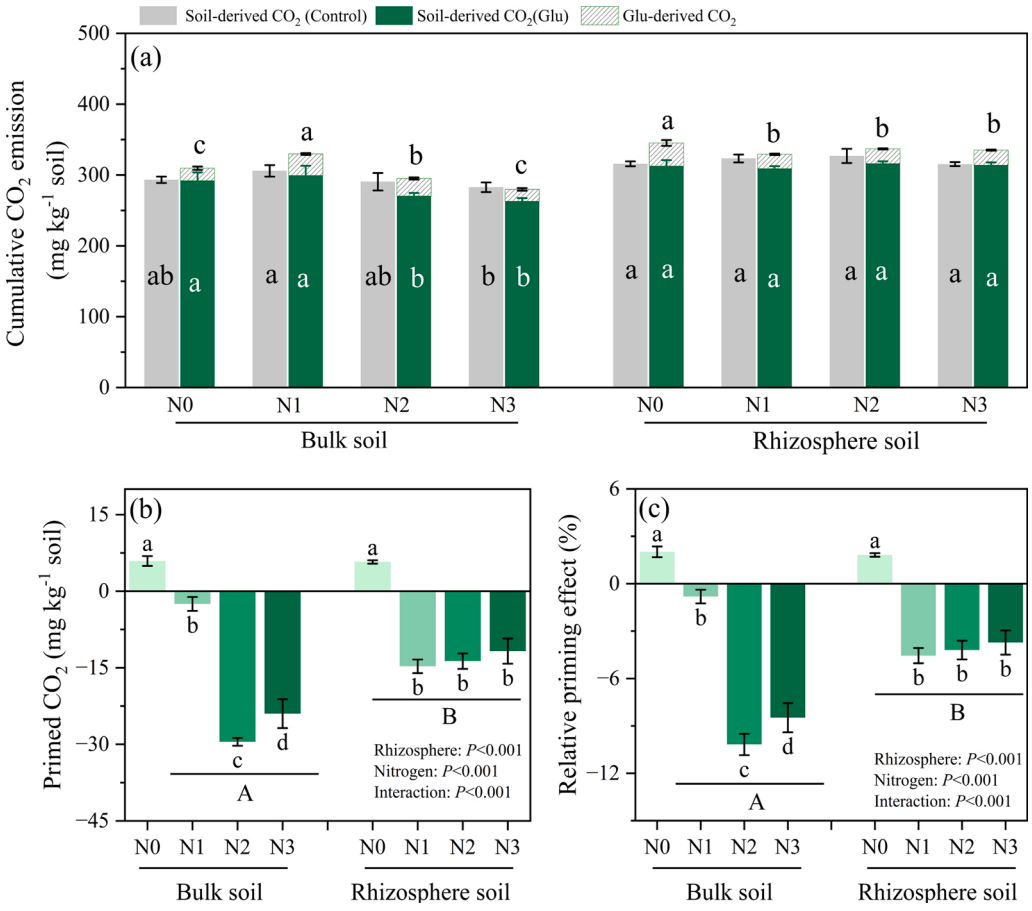

Fig. 1. Cumulative CO_2 emission (a), primed CO_2 (b) and relative priming effect (c) under the bulk and rhizosphere soils subjected to different nitrogen fertilization application rates over the 49-day incubation. Chemical N fertilizer treatments: N0 (0 kg chemical N ha^{-1}), N1 (102 kg chemical N ha^{-1}), N2 (327 kg chemical N ha^{-1}), N3 (552 kg chemical N ha^{-1}). Different lowercase letters indicate significant differences among different N fertilizer application rates at $P < 0.05$. Different uppercase letters indicate significant differences between bulk and rhizosphere soils at $P < 0.05$.

Table1
Soil physicochemical properties prior to incubation, following 15 years of chemical N fertilizer application.

	Bulk soils				Rhizosphere soils			
	N0	N1	N2	N3	N0	N1	N2	N3
pH	7.87 ± 0.03b	7.95 ± 0.03a	7.84 ± 0.03bc	7.81 ± 0.02c	8.12 ± 0.02a	7.99 ± 0.04b	7.99 ± 0.07b	7.79 ± 0.02c
SOC (g kg^{-1})	7.99 ± 0.50b	8.04 ± 0.42b	8.92 ± 0.30a	8.68 ± 0.51ab	6.99 ± 0.58b	8.07 ± 1.25ab	9.44 ± 0.24a	8.39 ± 0.90ab
TN (g kg^{-1})	1.21 ± 0.10a	1.31 ± 0.09a	1.32 ± 0.04a	1.40 ± 0.14a	1.11 ± 0.10b	1.22 ± 0.08ab	1.28 ± 0.08a	1.38 ± 0.06a
C:N ratio	6.60 ± 0.24a	6.15 ± 0.25a	6.75 ± 0.09a	6.23 ± 0.64a	6.31 ± 0.24b	6.56 ± 0.57ab	7.39 ± 0.65a	6.08 ± 0.45b
MN (mg kg^{-1})	25.28 ± 2.41c	21.31 ± 1.31c	35.46 ± 1.71b	98.50 ± 10.06a	21.79 ± 2.87c	26.64 ± 1.26c	51.84 ± 4.84b	57.67 ± 0.29a

SOC: soil organic carbon; TN: total nitrogen; C:N ratio: SOC to TN ratio; MN: mineral nitrogen (the sum of NH_4^+–N and NO_3^-–N);
N0: 0 kg chemical N ha^{-1}; N1: 102 kg chemical N ha^{-1}; N2: 327 kg chemical N ha^{-1}; N3: 552 kg chemical N ha^{-1}.

In bulk soils, microbial assimilation capacity significantly increased under N1 and N2 treatments compared with N0 treatment (Fig. 3a). Specifically, ^{13}PLFA, ^{13}Bacteria, $^{13}G^-$, and ^{13}Fungal increased by 50.1 %, 52.1 %, 70.4 %, and 40.4 % under N1 treatment, and by 65.0 %, 66.4 %, 113.3 %, and 54.2 % under N2 treatment, respectively. Similarly, $^{13}G^+$ increased by 37.3 % under N1 treatment and 24.2 % under N2 treatment. In contrast, microbial assimilation capacity under N3 treatment showed no significant difference except for $^{13}G^+$, which reduced by 21.2 % (Fig. 3a; $P < 0.05$).

Long-term N fertilizer application significantly increased glucose-derived MBC (^{13}MBC) by 3.3–7.0 times and CUE by 1.0–1.5 times compared with N0 treatment in bulk soils (Fig. 3bc; $P < 0.05$; Eqs. (5–7)). In rhizosphere soils, ^{13}MBC increased by 36.3 % under N3 treatment compared with N0 treatment. On average, ^{13}MBC decreased by 31.8 % and CUE increased by 10.9 % in bulk soils compared with rhizosphere soils (Fig. 3bc; $P < 0.05$; Eqs. (5–7)).

3.4. Factors controlling priming effect

Partial correlation analysis showed that the relative PE was negatively correlated with DON, CUE, ^{13}MBC, and BG, while it was positively correlated with MBC (Fig. 4). Random forest analysis indicated that soil N availability, microbial community, microbial assimilation capacity and enzyme activity explained of 22 %, 23 %, 22 % and 34 % of the total variance in relative PE, respectively (Fig. 5). The key variables regulating relative PE were BG (15 %), DOC:DON ratio (11 %), CUE (11 %) and DON (10 %) (Fig. 5). Furthermore, linear regression analysis also demonstrated relative PE was significantly increased with the DOC:DON

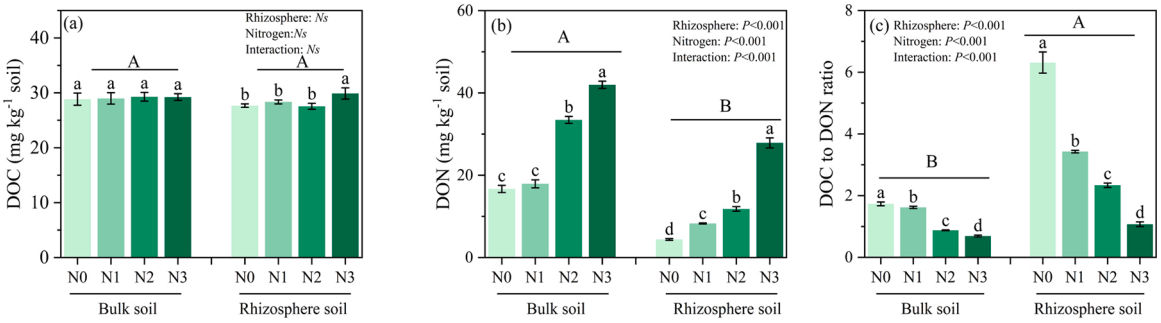

Fig. 2. Dissolved organic carbon content (DOC; a), Dissolved organic nitrogen content (DON; b) and dissolved organic carbon to dissolved organic nitrogen ratio (DOC to DON ratio; c) under the bulk and rhizosphere soils subjected to different nitrogen fertilization application over the 49-day incubation. Chemical N fertilizer treatments: N0 (0 kg chemical N ha^{-1}), N1 (102 kg chemical N ha^{-1}), N2 (327 kg chemical N ha^{-1}), N3 (552 kg chemical N ha^{-1}). Different lowercase letters indicate significant differences among different N fertilizer application rates at $P < 0.05$. Different uppercase letters indicate significant differences between bulk and rhizosphere soils at $P < 0.05$.

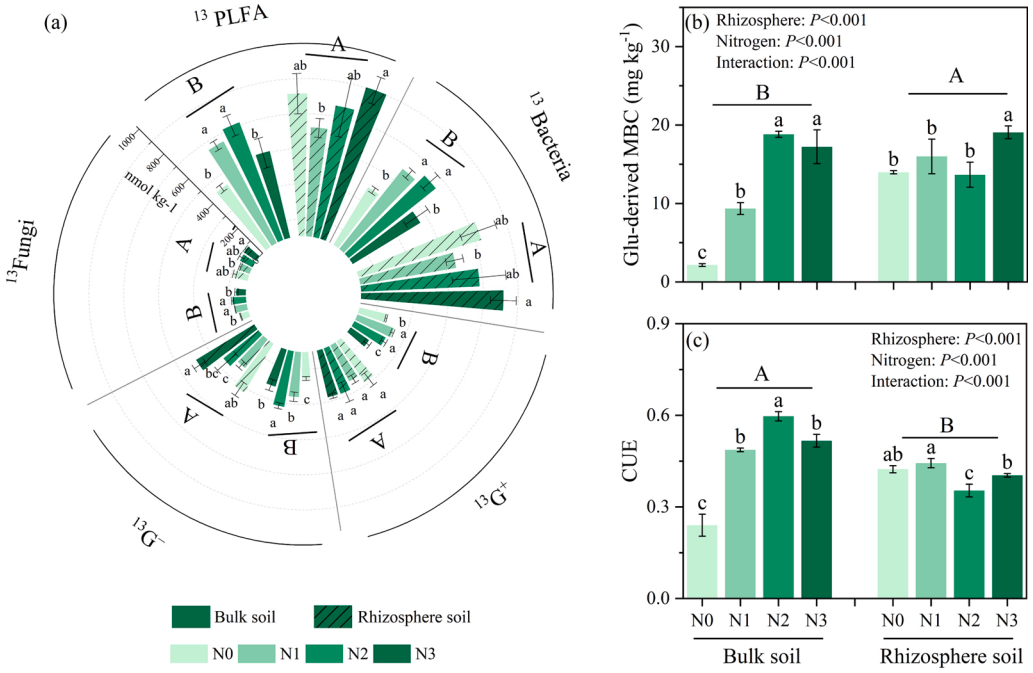

Fig. 3. Soil microbial assimilation capacity (a), ^{13}C-glucose-derived microbial biomass carbon (^{13}Glu-derived MBC; b) and microbial carbon use efficiency (CUE; c) under the bulk and rhizosphere soils subjected to different nitrogen fertilization application over the 49-day incubation. Chemical N fertilizer treatments: N0 (0 kg chemical N ha^{-1}), N1 (102 kg chemical N ha^{-1}), N2 (327 kg chemical N ha^{-1}), N3 (552 kg chemical N ha^{-1}). Reflects the utilization of added glucose, represented by ^{13}Fungi (^{13}C-labeled fungi), ^{13}Bacteria (^{13}C-labeled bacteria), $^{13}G^{+}$ (^{13}C-labeled gram-positive bacteria), $^{13}G^{-}$ (^{13}C-labeled gram-negative bacteria). Different lowercase letters indicate significant differences among different N fertilizer application rates at $P < 0.05$. Different uppercase letters indicate significant differences between bulk and rhizosphere soils at $P < 0.05$.

ratio (R^2=0.32, $P < 0.01$; Fig. 5b), whereas significantly decreased with CUE (R^2=0.51, $P < 0.001$; Fig. 5d) and BG activity (R^2=0.41, $P < 0.001$; Fig. 5e).

The PLS-PM analysis further confirmed the results, revealing that soil N availability indirectly regulated relative PE through microbial community, microbial assimilation capacity and enzyme activity (Fig. 6a). Together, these factors collectively explained 89 % of the variance in the relative PE. The microbial community (path coefficient = +0.50), microbial assimilation capacity (path coefficient = –0.54) and enzyme activity (path coefficient = –0.66) showed strong direct effects on relative PE.

4. Discussion

4.1. Priming effect was controlled by N fertilizer application

The PE was strongly modulated by long-term nitrogen (N) fertilization (Fig. 1). In this study, we employed ^{13}C-labeled glucose as a tracer to distinguish exogenous carbon (simulated root exudates) and native SOC mineralization. Our result showed that long-term N fertilizer application (N1, N2, and N3 treatments) induced significant negative PE and relative PE (PE < 0) in soil niches (rhizosphere vs. bulk soil), whereas the N0 treatment showed most pronounced positive PE (PE > 0)

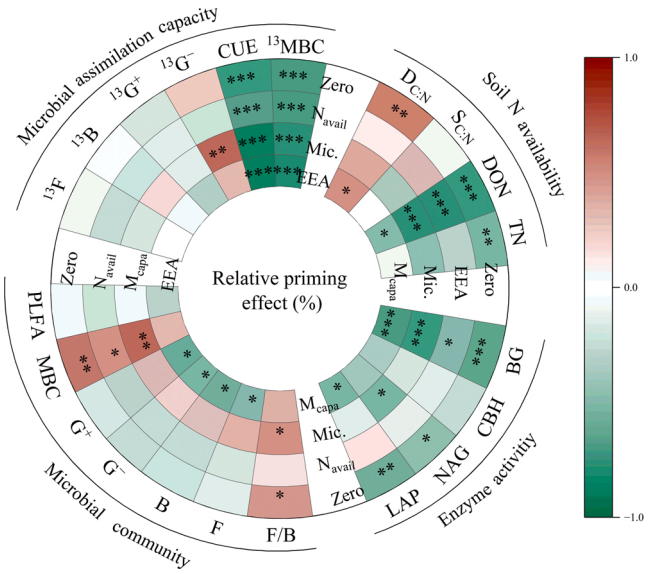

Fig. 4. Partial correlation analysis of the relative priming effect (RPE) and key soil and microbial properties. The heatmap shows the independent relationships between RPE and soil nitrogen availability (Navail), microbial properties (Mic.), soil extracellular enzyme activity (EEA), and microbial assimilation capacity (Mcapa). Nitrogen availability (Navail): Includes $D_{C:N}$ (the ratio of dissolved organic carbon to dissolved organic nitrogen), $S_{C:N}$ (the ratio of soil organic carbon to total nitrogen), DON (dissolved organic nitrogen), and TN (total nitrogen). Microbial properties (Mic): Comprises PLFA (phospholipid fatty acids), MBC (microbial biomass carbon), G^+ (gram-positive bacteria), G^- (gram-negative bacteria), B (bacteria), F (fungi), and F/B (the fungi-to-bacteria ratio). Extracellular enzyme activity (EEA): Includes BG (β-1,4-glucosidase), CBH (cellobiohydrolase), LAP (leucine aminopeptidase), and NAG (β-N-acetylglucosaminidase), representing enzymes involved in carbon and nitrogen acquisition. Microbial assimilation capacity (Mcapa): Reflects the utilization of added glucose, represented by ^{13}F (^{13}C-labeled fungi), ^{13}B (^{13}C-labeled bacteria), $^{13}G^+$ (^{13}C-labeled gram-positive bacteria), $^{13}G^-$ (^{13}C-labeled gram-negative bacteria), ^{13}F/B (the ratio of ^{13}C-labeled fungi to bacteria), ^{13}MBC (^{13}C-labeled microbial biomass carbon), and CUE (carbon use efficiency). The heatmap shows correlation strength, with red indicating positive and green negative correlations. Significance levels are indicated by $^*P < 0.05$, $^{**}P < 0.01$, and $^{***}P < 0.001$.

in both soil niches (Fig. 1b, c). These contrasting responses can be explained by two complementary mechanisms. Under the N0 condition, the addition of labile carbon likely triggered microbial N mining from SOC, consistent with the nitrogen mining hypothesis (Craine et al., 2007; Fontaine et al., 2011). In N0 treatment, microbes experience N limitation, resulting certain K-strategist microbes are stimulated to produce extracellular enzymes to mine nitrogen from soil organic matter (SOM), leading to enhanced SOC mineralization and a positive PE. (Craine et al., 2007; Fontaine et al., 2011; Lyu et al., 2019). In contrast, under nitrogen-fertilized conditions (N1–N3) the observed negative PE aligns with the preferential substrate utilization hypothesis, which proposes that microbes preferentially assimilate added labile carbon (e.g., glucose) instead of decomposing native SOC (Kuzyakov, 2010; Cheng et al., 2014; Bei et al., 2022). Additionally, nitrogen addition increases soil N availability, reducing microbial demand for N acquisition from SOC (Li et al., 2023; Yang et al., 2024), further suppressing SOC mineralization. Together, these mechanisms explain the shift in PE direction from positive under N deficiency to negative under N enrichment. These mechanisms are supported by microbial community structure data (Fig. 3a) and DON dynamics (Fig. 2). Compared with N0 treatment, the N1 and N2 treatments significantly enhanced microbial assimilation of exogenous ^{13}C-glucose, as indicated by increased ^{13}PLFA, ^{13}Bacteria, ^{13}Fungi, $^{13}G^-$ and $^{13}G^+$ (Fig. 3a). At the same time, DON content increased and the DOC:DON ratio decreased under long-term N application (Fig. 2), indicating improved N availability. This shift in resource availability stimulated microbial growth and increased CUE (Fig. 3c), leading to greater incorporation of exogenous carbon into biomass (^{13}MBC; Fig. 3b) and reduced SOC mineralization. Consistently, negative correlations between relative PE and both ^{13}MBC and CUE (Fig. 4) support previous findings that increased microbial mobilization of glucose-derived C can lead to stronger negative PE (Su and Shangguan, 2023). Overall, these findings confirm that long-term N fertilizer application enhances soil carbon stability by reducing PE through suppressing SOC mineralization (Kuzyakov, 2010; Nottingham et al., 2015; Hicks et al., 2019; Chen et al., 2021; Feng et al., 2021).

Despite all N treatments suppressing PE, their effects varied by dose. In bulk soil, the strongest negative PE was observed under N2, followed by N3 and N1 (Fig. 1b, c). Under N1, limited nitrogen availability likely constrained microbial metabolism, resulting in lower ^{13}MBC (Fig. 3b) and higher CO_2 emissions (Fig. 3b, Fig. 1a). This led to a significant decline in CUE (Fig. 3c), suggesting that microbes were less efficient in assimilating added glucose, resulting in the weakest suppression of PE among the N treatments. In contrast, the N2 treatment improved microbial nutrient balance by increasing DON and lowering the DOC:DON ratio (Fig. 2b), thereby enhancing microbial growth and carbon assimilation rather than respiration (Manzoni et al., 2012; Michel et al., 2023). The microbial community shifted toward bacterial groups (e.g., $^{13}G^+$, $^{13}G^-$) that efficiently utilized labile carbon. Consequently, more glucose-derived carbon was incorporated into microbial biomass (^{13}MBC, ^{13}PLFA; Fig. 3b), CUE increased (Fig. 3c), and SOC mineralization was more strongly suppressed, resulting in the strongest negative PE, these findings align with the view that labile carbon sources promote microbial anabolism over catabolism (Fontaine et al., 2003, 2011; Chen et al., 2019). However, despite even higher DON levels under N3 treatment (Fig. 2b), the negative PE was weaker than under N2, likely due to impaired microbial carbon assimilation capacity. Microbial CUE significantly declined compared to N2 treatment (Fig. 3c) and $^{13}G^+$ also decreased (Fig. 3a), indicating reduced microbial anabolic activity. These changes suggest that excess N may have impaired microbial function and shifted the community toward fast-growing, copiotrophic r-strategists (e.g., $^{13}G^-$) (Zhang et al., 2023; Wang et al., 2024a). Such microbes tend to inefficiently assimilate carbon, potentially allocating more C toward non-growth-related processes, thereby weakening the microbial capacity to suppress SOC mineralization and reducing the negative PE effect (Blagodatskaya and Kuzyakov, 2008; Averill and Waring, 2018). In addition, the significant decline in rhizosphere pH under N3 treatment (Table 1) compared with N0 treatments may also have contributed to this negative PE. As shown in the correlation heatmap (Fig. S4), pH was strongly negatively correlated with enzyme activities (BG, NAG, LAP), suggesting that acidification could alter microbial enzymatic function. However, pH showed limited associations with microbial traits, being positively correlated only with $^{13}G^+$ abundance. Although pH is the environmental variables most closely associated with soil microbial community composition and metabolism (Crocker et al., 2024; Lee et al., 2025), its overall effect on microbial carbon assimilation appeared to be minor in our system.

Radom forest and Partial least squares path modeling (PLS-PM, Fig. 5 and Fig. 6) further supported these mechanisms, indicating that ^{13}MBC, CUE, and enzyme activity were the main drivers of PE, rather than native soil-derived microbial communities. Notably, increased enzyme activities (Fig. S3) under N treatments facilitated more efficient glucose utilization rather than enhancing SOC decomposition. These findings suggest that long-term N fertilization suppresses PE by improving N availability and promoting microbial traits that promote the assimilation of labile carbon, thus protecting native SOC.

4.2. The priming effect in the rhizosphere soils

Interestingly, although N fertilization consistently induced negative PE across all N treatments, the degree of PE suppression was

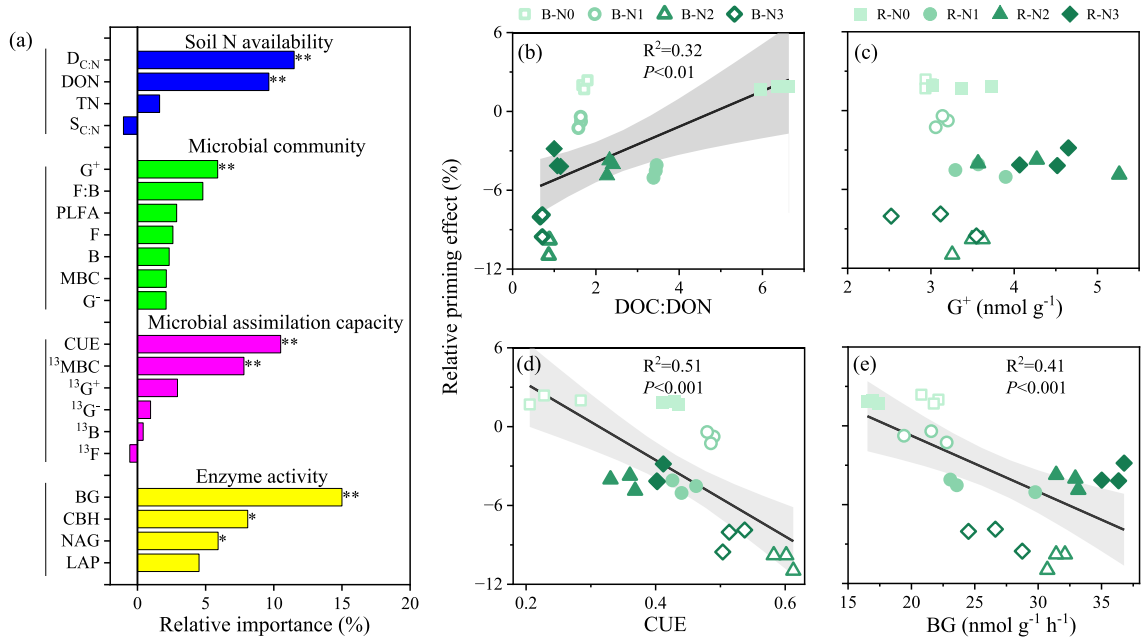

Fig. 5. The importance for soil relative priming effect (PE, a) and its linear relationship with DON:DOC, G^+, CUE and BG (b, c, d and e). The relative importance was selected by random forest analysis. The estimation of the importance of predictors was based on the percentage increases in mean squared error (MSE). Variables with higher MSE% values were identified as more importance. Nitrogen availability (Navail): Includes $D_{C:N}$ (the ratio of dissolved organic carbon to dissolved organic nitrogen), $S_{C:N}$ (the ratio of soil organic carbon to total nitrogen), DON (dissolved organic nitrogen), and TN (total nitrogen). Microbial properties (Mic): Comprises PLFA (phospholipid fatty acids), MBC (microbial biomass carbon), G^+ (gram-positive bacteria), G^- (gram-negative bacteria), B (bacteria), F (fungi), and F/B (the fungi-to-bacteria ratio). Extracellular enzyme activity (EEA): Includes BG (β-1,4-glucosidase), CBH (cellobiohydrolase), LAP (leucine aminopeptidase), and NAG (β-N-acetylglucosaminidase), representing enzymes involved in carbon and nitrogen acquisition. Microbial assimilation capacity (Mcapa): Reflects the utilization of added glucose, represented by ^{13}F (^{13}C-labeled fungi), ^{13}B (^{13}C-labeled bacteria), $^{13}G^+$ (^{13}C-labeled gram-positive bacteria), $^{13}G^-$ (^{13}C-labeled gram-negative bacteria), $^{13}F/B$ (the ratio of ^{13}C-labeled fungi to bacteria), ^{13}MBC (^{13}C-labeled microbial biomass carbon), and CUE (carbon use efficiency). Significance levels are indicated by $^*P < 0.05$, $^{**}P < 0.01$, and $^{***}P < 0.001$.

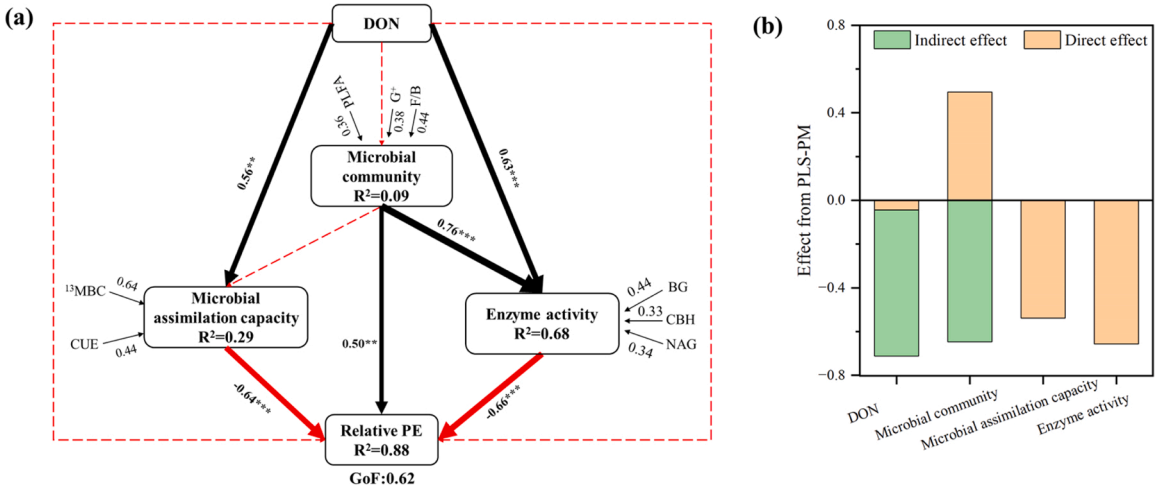

Fig. 6. (a) Partial least squares path modeling (PLS-PM) showing how nitrogen fertilizer direct and indirect effects affected relative priming effect via microbial community structure and microbial function (microbial assimilation capacity and enzyme activity). Larger path coefficients were shown as wider arrows, while black and red lines indicate positive and negative effects, solid and dotted lines indicate significant and insignificant effects, respectively. Path coefficients were calculated after 1000 bootstraps and significance is indicated by an asterisk ($^*P < 0.05$, $^{**}P < 0.01$, and $^{***}P < 0.001$.). The GoF value was 0.62. (b) Standardized direct and indirect effects on relative priming effect derived from the PLS-PM.

significantly weaker in rhizosphere soils compared with bulk soils (Fig. 1b, c). This finding indicates that the effect of N fertilization on SOC mineralization is modulated by soil niches (rhizosphere or bulk soil). Specifically, PE intensity varied significantly among N1–N3 treatments in bulk soils but remained relatively unchanged in the rhizosphere soils (Fig. 1c), suggesting that the rhizosphere environment buffers microbial responses to increasing N availability. This buffering capacity may be explained as the stimulatory effect of microbial activity by the unique biochemical environment of the rhizosphere (Kuzyakov et al., 2000). Our data showed significantly higher microbial biomass (as indicated by PLFAs) and greater assimilation of exogenous (^{13}PLFA) in rhizosphere soils compared with bulk soils (Fig. 3a, b). Although N fertilization suppressed PE, the continuous release of root exudates likely stimulated microbial activity in the rhizosphere, partially counteract the

suppressive effect of N fertilization on SOC mineralization (Cheng et al., 2014; Finzi et al., 2015).

Additionally, the significantly reduced CUE observed in rhizosphere soils suggests that microbial communities allocate a greater proportion of carbon toward respiration rather than growth, possibly to meet the heightened metabolic demands driven by intense nutrient competition with plant roots (Fontaine et al., 2011). Although our experiment was conducted without living plants, the rhizosphere soils may retain functional imprints of prior plant–microbe interactions This is reflected in the distinct microbial community composition (Fig. S2) and higher incorporation of glucose-derived C (Fig. 3a, b), suggesting that microbial community remains adapted to root-derived carbon. Such legacy effects, although not directly measured, may help explain the relatively stable PE in the rhizosphere under increased soil N availability. The use of ^{13}C-labeled glucose in this study served as a simplified model of rhizodeposition, allowing us to examine microbial responses to labile carbon under varying N inputs. However, in natural systems, long-term N fertilization can alter root exudation patterns, which may further influence microbial community composition and PE response. Therefore, the observed divergence in PE between rhizosphere and bulk soils likely reflects both microbial physiological regulation and plant-mediated legacy effects.

Bulk soils exhibited a significantly stronger negative PE (-12.5 mg kg^{-1} soil) compared with rhizosphere soils (-8.6 mg kg^{-1} soil; $P < 0.05$, Fig. 1). This phenomenon is likely attributable to a significant reduction of N availability in rhizosphere soils relative to bulk soils (Yin et al., 2021), as evidenced by the negative correlation between soil N availability and relative PE intensity (Fig. 6). In addition, rhizosphere microbial communities experience enhanced N limitation due to substantial deposition of root-exuded carbon, which intensifies microbial demand for N resources (Lian et al., 2024). Moreover, continuous N uptake by plant leads to lower DON content and a higher DOC: DON ratio in rhizosphere soil (Fig. 2). The supplementation of liable carbon trough glucose addition further stimulates microbial growth and activity by activating dormant microbial taxa, as indicated by the significant increase in PLFAs contents (Fig. S2). The greater microbial abundance and activity in the rhizosphere soils increases the demand for energy and nutrients to support growth and metabolism (He et al., 2023; Qin et al., 2024), which in turn enhances PE. These findings collectively support our second and third hypotheses, emphasizing that (i) rhizosphere soils exhibit stronger PE than bulk soils due to higher microbial activity and N limitation, and (ii) the interaction between N fertilization and soil niches plays a critical role in modulating the magnitude and direction of PE.

Collectively, these findings indicate that rhizosphere soils exhibit a lower capacity than bulk soils to mitigate glucose-induced SOC priming and promote SOC sequestration in GVP systems. However, it is important to recognize the limitations of using glucose as a sole proxy representative of root exudates. While glucose addition offers a controlled approach to trace microbial C utilization, natural root exudates are chemically diverse, comprising a mixture of sugars, organic acids, amino acids, and secondary metabolites. These compounds interact with microbial communities in more complex ways than glucose alone, potentially modulating PE through multiple microbial pathways (Fu et al., 2025). Therefore, the weaker negative priming effect observed in rhizosphere soils may not only reflect microbial responses to glucose, but also be shaped by the broader biochemical landscape of the rhizosphere. This limitation should be considered when extrapolating our findings to field-scale rhizosphere C cycling. Moreover, our findings underscore the importance of the interaction between long-term N fertilization and soil niche, as the strength and direction of priming effects varied across rhizosphere and bulk soils under different N regimes. Such interactions should be emphasized when designing fertilization strategies aimed at enhancing SOC stability in cropping systems.

5. Conclusion

Our findings demonstrate that under consistent organic inputs, long-term chemical N fertilization, soil niches (rhizosphere vs. bulk soil), and their interaction collectively regulate SOC turnover by altering the direction and magnitude of glucose-induced PE. Across all chemical N treatments (N1–N3), negative PE was observed, indicating that increased N availability suppresses native SOC mineralization, primarily through shifts in microbial community composition and metabolic strategies, including enhanced carbon assimilation (CUE,^{13}MBC) and enzyme activity (BG, CBH, NAG). However, rhizosphere soils consistently exhibited weaker negative PE than bulk soils, suggesting that the rhizosphere partially counteracts the suppression of PE induced by N fertilization. This response is driven by microbial legacy effects and nutrient dynamics—particularly reduced DON levels from prior plant uptake, which sustain microbial activity and promote continued SOC decomposition. Despite higher ^{13}C incorporation into microbial biomass (e.g.,^{13}C-PLFA, ^{13}MBC) in the rhizosphere, elevated CO_2 emissions and lower CUE suggest that microbes preferentially respired glucose rather than investing it into biomass, thereby weakening negative PE and limiting SOC protection. These findings underscore a clear interaction between N fertilization and soil niche, highlighting that the rhizosphere's distinct biochemical and microbial characteristics can override fertilization effects. Therefore, effective N management should consider not only the amount of N applied, but also plant-mediated spatial heterogeneity to optimize SOC stability in greenhouse vegetable systems.

CRediT authorship contribution statement

Jianfeng Zhang: Resources, Project administration, Funding acquisition, Conceptualization. **Guihua Li:** Writing – review & editing, Supervision, Funding acquisition, Conceptualization. **Sébastien Massart:** Writing – review & editing, Supervision. **Jinshan Lian:** Writing – original draft, Methodology, Investigation, Conceptualization.

Declaration of Competing Interest

The authors declare that they have no known competing financial interests or personal relationships that could have appeared to influence the work reported in this paper.

Acknowledgements

We acknowledge all the colleagues for their unremitting efforts on the long-term experiments. We also sincerely thank Dr. Xiao Liu for her valuable help in improving the English language of this manuscript. This research was funded by the National Natural Science Foundation of China (grant number: 22176215), the Earmarked fund for CARS (grant number: CARS 23-B18), Key Technology Research and Development Program of Shandong Province (grant number: 2023TZXD087) and the program of China Scholarship Council (grant number:202303250059).

Appendix A. Supporting information

Supplementary data associated with this article can be found in the online version at doi:10.1016/j.still.2025.106802.

Data availability

Data will be made available on request.

References

Averill, C., Waring, B., 2018. Nitrogen limitation of decomposition and decay: how can it occur? Glob. Chang Biol. 24, 1417–1427. https://doi.org/10.1111/gcb.13980.

Aye, N.S., Butterly, C.R., Sale, P.W.G., Tang, C., 2018. Interactive effects of initial ph and nitrogen status on soil organic carbon priming by glucose and lignocellulose. Soil Biol. Biochem. 123, 33–44. https://doi.org/10.1016/j.soilbio.2018.04.027.

Bei, S., Li, X., Kuyper, T.W., Chadwick, D.R., Zhang, J., 2022. Nitrogen availability mediates the priming effect of soil organic matter by preferentially altering the straw carbon-assimilating microbial community. Sci. Total Environ. 815, 152882. https://doi.org/10.1016/j.scitotenv.2021.152882.

Blagodatskaya, E., Kuzyakov, Y., 2008. Mechanisms of real and apparent priming effects and their dependence on soil microbial biomass and community structure: a critical review. Biol. Fertil. Soils 45, 115–131. https://doi.org/10.1007/s00374-008-0334-y.

Bremner, J.M., Mulvaney, C.S., 1983. Nitrogen-Total, in: methods of soil analysis. Agron. Monogr. 595–624. https://doi.org/10.2134/agronmonogr9.2.2ed.c31.

Chen, P., Mo, C., He, C., Cui, H., Lin, J., Yang, J., 2021. Shift of microbial turnover time and metabolic efficiency strongly regulates rhizosphere priming effect under nitrogen fertilization in paddy soil. Sci. Total Environ. 800, 149590. https://doi.org/10.1016/j.scitotenv.2021.149590.

Chen, S., Waghmode, T.R., Sun, R., Kuramae, E.E., Hu, C., Liu, B., 2019. Root-associated microbiomes of wheat under the combined effect of plant development and nitrogen fertilization. Microbiome 7, 136. https://doi.org/10.1186/s40168-019-0750-2.

Cheng, W., Parton, W.J., Gonzalez-Meler, M.A., Phillips, R., Asao, S., McNickle, G.G., Brzostek, E., Jastrow, J.D., 2014. Synthesis and modeling perspectives of rhizosphere priming. New Phytol. 201, 31–44. https://doi.org/10.1111/nph.12440.

Craine, J.M., Morrow, C., Fierer, N., 2007. Microbial nitrogen limitation increases decomposition. Ecology 88, 2105–2113. https://doi.org/10.1890/06-1847.1.

Crocker, K., Lee, K.K., Chakraverti-Wuerthwein, M., Li, Z., Tikhonov, M., Mani, M., Gowda, K., Kuehn, S., 2024. Environmentally dependent interactions shape patterns in gene content across natural microbiomes. Nat. Microbiol. 9, 2022–2037. https://doi.org/10.1038/s41564-024-01752-4.

Dai, Z., Su, W., Chen, H., Barberán, A., Zhao, H., Yu, M., Yu, L., Brookes, P.C., Schadt, C. W., Chang, S.X., Xu, J., 2018. Long-term nitrogen fertilization decreases bacterial diversity and favors the growth of actinobacteria and proteobacteria in agro-ecosystems across the globe. Glob. Chang Biol. 24, 3452–3461. https://doi.org/10.1111/gcb.14163.

Domeignoz-Horta, L.A., Pold, G., Liu, X.-J.A., Frey, S.D., Melillo, J.M., DeAngelis, K.M., 2020. Microbial diversity drives carbon use efficiency in a model soil. Nat. Commun. 11, 3684. https://doi.org/10.1038/s41467-020-17502-z.

Edwards, J., Johnson, C., Santos-Medellín, C., Lurie, E., Podishetty, N.K., Bhatnagar, S., Eisen, J.A., Sundaresan, V., 2015. Structure, variation, and assembly of the root-associated microbiomes of rice. Proc. Natl. Acad. Sci. 112, E911–E920. https://doi.org/10.1073/pnas.1414592112.

Fang, Y., Nazaries, L., Singh, B.K., Singh, B.P., 2018. Microbial mechanisms of carbon priming effects revealed during the interaction of crop residue and nutrient inputs in contrasting soils. Glob. Change Biol. 24, 2775–2790. https://doi.org/10.1111/gcb.14154.

Feng, J., Zhu, B., 2021. Global patterns and associated drivers of priming effect in response to nutrient addition. Soil Biol. Biochem. 153, 108118. https://doi.org/10.1016/J.SOILBIO.2020.108118.

Feng, J., Tang, M., Zhu, B., 2021. Soil priming effect and its responses to nutrient addition along a tropical forest elevation gradient. Glob. Chang Biol. 27, 2793–2806. https://doi.org/10.1111/gcb.15587.

Finn, D., Page, K., Catton, K., Strounina, E., Kienzle, M., Robertson, F., Armstrong, R., Dalal, R., 2015. Effect of added nitrogen on plant litter decomposition depends on initial soil carbon and nitrogen stoichiometry. Soil Biol. Biochem. 91, 160–168. https://doi.org/10.1016/j.soilbio.2015.09.001.

Finzi, A.C., Abramoff, R.Z., Spiller, K.S., Brzostek, E.R., Darby, B.A., Kramer, M.A., Phillips, R.P., 2015. Rhizosphere processes are quantitatively important components of terrestrial carbon and nutrient cycles. Glob. Change Biol. 21, 2082–2094. https://doi.org/10.1111/gcb.12816.

Fontaine, S., Mariotti, A., Abbadie, L., 2003. The priming effect of organic matter: a question of microbial competition? Soil Biol. Biochem. 35, 837–843. https://doi.org/10.1016/S0038-0717(03)00123-8.

Fontaine, S., Henault, C., Aamor, A., Bdioui, N., Bloor, J.M.G., Maire, V., Mary, B., Revaillot, S., Maron, P.A., 2011. Fungi mediate long term sequestration of carbon and nitrogen in soil through their priming effect. Soil Biol. Biochem. 43, 86–96. https://doi.org/10.1016/J.SOILBIO.2010.09.017.

Fu, Y., Liu, W., Chen, Z., Redmile-Gordon, M., Liang, C., Tang, C., Guggenberger, G., Yan, S., Yin, L., Peng, J., Van Zwieten, L., Wang, P., Chen, J., Kuzyakov, Y., Ge, T., Xu, J., Luo, Y., 2025. Microbial metabolisms determine soil priming effect induced by organic inputs. Soil Biol. Biochem., 109885 https://doi.org/10.1016/j.soilbio.2025.109885.

Geisseler, D., Scow, K.M., 2014. Long-term effects of mineral fertilizers on soil microorganisms – a review. Soil Biol. Biochem. 75, 54–63. https://doi.org/10.1016/j.soilbio.2014.03.023.

Gunina, A., Kuzyakov, Y., 2015. Sugars in soil and sweets for microorganisms: review of origin, content, composition and fate. Soil Biol. Biochem. 90, 87–100. https://doi.org/10.1016/j.soilbio.2015.07.021.

He, C., Harindintwali, J.D., Cui, H., Cui, Y., Chen, P., Mo, C., Zhu, Q., Zheng, W., Alessi, D.S., Wang, F., Jiang, Z., Yang, J., 2023. Deciphering the dual role of bacterial communities in stabilizing rhizosphere priming effect under intra-annual change of growing seasons. Sci. Total Environ. 903, 166777. https://doi.org/10.1016/j.scitotenv.2023.166777.

Hicks, L.C., Meir, P., Nottingham, A.T., Reay, D.S., Stott, A.W., Salinas, N., Whitaker, J., 2019. Carbon and nitrogen inputs differentially affect priming of soil organic matter in tropical lowland and montane soils. Soil Biol. Biochem. 129, 212–222. https://doi.org/10.1016/J.SOILBIO.2018.10.015.

Jia, X., Zhong, Y., Liu, J., Zhu, G., Shangguan, Z., Yan, W., 2020. Effects of nitrogen enrichment on soil microbial characteristics: from biomass to enzyme activities. Geoderma 366, 114256. https://doi.org/10.1016/j.geoderma.2020.114256.

Kachurina, O.M., Zhang, H., Raun, W.R., Krenzer, E.G., 2000. Simultaneous determination of soil aluminum, ammonium- and nitrate-nitrogen using 1 m potassium chloride extraction. Commun. Soil Sci. Plant Anal. 31, 893–903. https://doi.org/10.1080/00103620009370485.

Kianpoor Kalkhajeh, Y., Huang, B., Hu, W., Ma, C., Gao, H., Thompson, M.L., Bruun Hansen, H.C., 2021. Environmental soil quality and vegetable safety under current greenhouse vegetable production management in China. Agric. Ecosyst. Environ. 307, 107230. https://doi.org/10.1016/j.agee.2020.107230.

Kuzyakov, Y., 2010. Priming effects: interactions between living and dead organic matter. Soil Biol. Biochem. 42, 1363–1371. https://doi.org/10.1016/J.SOILBIO.2010.04.003.

Kuzyakov, Y., Blagodatskaya, E., 2015. Microbial hotspots and hot moments in soil: concept & review. Soil Biol. Biochem. 83, 184–199. https://doi.org/10.1016/j.soilbio.2015.01.025.

Kuzyakov, Y., Xu, X., 2013. Competition between roots and microorganisms for nitrogen: mechanisms and ecological relevance. New Phytol. 198, 656–669. https://doi.org/10.1111/nph.12235.

Kuzyakov, Y., Friedel, J.K., Stahr, K., 2000. Review of mechanisms and quantification of priming effects. Soil Biol. Biochem. 32, 1485–1498. https://doi.org/10.1016/S0038-0717(00)00084-5.

Lee, K.K., Liu, S., Crocker, K., Wang, J., Huggins, D.R., Tikhonov, M., Mani, M., Kuehn, S., 2025. Functional regimes define soil microbiome response to environmental change. Nature. https://doi.org/10.1038/s41586-025-09264-9.

Lenka, S., Trivedi, P., Singh, B., Singh, B.P., Pendall, E., Bass, A., Lenka, N.K., 2019. Effect of crop residue addition on soil organic carbon priming as influenced by temperature and soil properties. Geoderma 347, 70–79. https://doi.org/10.1016/J.GEODERMA.2019.03.039.

Li, J., Yuan, X., Ge, L., Li, Q., Li, Z., Wang, L., Liu, Y., 2020. Rhizosphere effects promote soil aggregate stability and associated organic carbon sequestration in rocky areas of desertification. Agric. Ecosyst. Environ. 304, 107126. https://doi.org/10.1016/j.agee.2020.107126.

Li, Q., Shi, J., Li, G., Hu, J., Ma, R., 2023. Extracellular enzyme stoichiometry and microbial resource limitation following various grassland reestablishment in abandoned cropland. Sci. Total Environ. 870. https://doi.org/10.1016/j.scitotenv.2023.161746.

Lian, J., Li, G., Zhang, J., Massart, S., 2024. Nitrogen fertilization affected microbial carbon use efficiency and microbial resource limitations via root exudates. Sci. Total Environ. 950, 174933. https://doi.org/10.1016/j.scitotenv.2024.174933.

Liang, L., Ridoutt, B.G., Lal, R., Wang, D., Wu, W., Peng, P., Hang, S., Wang, L., Zhao, G., 2019. Nitrogen footprint and nitrogen use efficiency of greenhouse tomato production in north China. J. Clean. Prod. 208, 285–296. https://doi.org/10.1016/j.jclepro.2018.10.149.

Liu, X., Lu, X., Zhao, W., Yang, S., Wang, J., Xia, H., Wei, X., Zhang, J., Chen, L., Chen, Q., 2022. The rhizosphere effect of native legume albizzia julibrissin on coastal saline soil nutrient availability, microbial modulation, and aggregate formation. Sci. Total Environ. 806, 150705. https://doi.org/10.1016/j.scitotenv.2021.150705.

Luo, R., Kuzyakov, Y., Liu, D., Fan, J., Luo, J., Lindsey, S., He, J.-S., Ding, W., 2020. Nutrient addition reduces carbon sequestration in a Tibetan grassland soil: disentangling microbial and physical controls. Soil Biol. Biochem. 144, 107764. https://doi.org/10.1016/j.soilbio.2020.107764.

Lyu, M., Xie, J., Giardina, C.P., Vadeboncoeur, M.A., Feng, X., Wang, M., Ukonmaanaho, L., Lin, T.-C., Kuzyakov, Y., Yang, Y., 2019. Understory ferns alter soil carbon chemistry and increase carbon storage during reforestation with native pine on previously degraded sites. Soil Biol. Biochem. 132, 80–92. https://doi.org/10.1016/j.soilbio.2019.02.004.

Ma, T., Zhan, Y., Chen, W., Hou, Z., Chai, S., Zhang, J., Zhang, X., Wang, R., Liu, R., Wei, Y., 2024. Microbial traits drive soil priming effect in response to nitrogen addition along an alpine forest elevation gradient. Sci. Total Environ. 907, 167970. https://doi.org/10.1016/j.scitotenv.2023.167970.

Manzoni, S., Taylor, P., Richter, A., Porporato, A., Ågren, G.I., 2012. Environmental and stoichiometric controls on microbial carbon-use efficiency in soils. New Phytol. 196, 79–91. https://doi.org/10.1111/j.1469-8137.2012.04225.x.

Meyer, N., Welp, G., Rodionov, A., Borchard, N., Martius, C., Amelung, W., 2018. Nitrogen and phosphorus supply controls soil organic carbon mineralization in tropical topsoil and subsoil. Soil Biol. Biochem. 119, 152–161. https://doi.org/10.1016/j.soilbio.2018.01.024.

Michel, J., Hartley, I.P., Buckeridge, K.M., van Meegen, C., Broyd, R.C., Reinelt, L., Ccahuana Quispe, A.J., Whitaker, J., 2023. Preferential substrate use decreases priming effects in contrasting treeline soils. Biogeochemistry 162, 141–161. https://doi.org/10.1007/s10533-022-00996-8.

Nottingham, A.T., Turner, B.L., Stott, A.W., Tanner, E.V.J., 2015. Nitrogen and phosphorus constrain labile and stable carbon turnover in lowland tropical forest soils. Soil Biol. Biochem. 80, 26–33. https://doi.org/10.1016/j.soilbio.2014.09.012.

Olsen, S.R., Sommers, L.E., 1983. Phosphorus, in: methods of soil analysis. Agron. Monogr. 403–430. https://doi.org/10.2134/agronmonogr9.2.2ed.c24.

Pausch, J., Kuzyakov, Y., 2018. Carbon input by roots into the soil: quantification of rhizodeposition from root to ecosystem scale. Glob. Change Biol. 24, 1–12. https://doi.org/10.1111/gcb.13850.

Qin, W., Feng, J., Zhang, Q., Yuan, X., Zhou, H., Zhu, B., 2024. Nitrogen and phosphorus addition mediate soil priming effects via affecting microbial stoichiometric balance in an alpine meadow. Sci. Total Environ. 908, 168350. https://doi.org/10.1016/j.scitotenv.2023.168350.

Rocci, K.S., Cleveland, C.C., Eastman, B.A., Georgiou, K., Grandy, A.S., Hartman, M.D., Hauser, E., Holland-Moritz, H., Kyker-Snowman, E., Pierson, D., Reich, P.B., Schlerman, E.P., Wieder, W.R., 2024. Aligning theoretical and empirical representations of soil carbon-to-nitrogen stoichiometry with process-based terrestrial biogeochemistry models. Soil Biol. Biochem. 189, 109272. https://doi.org/10.1016/j.soilbio.2023.109272.

Schmidt, M.W.I., Torn, M.S., Abiven, S., Dittmar, T., Guggenberger, G., Janssens, I.A., Kleber, M., Kögel-Knabner, I., Lehmann, J., Manning, D.A.C., Nannipieri, P., Rasse, D.P., Weiner, S., Trumbore, S.E., 2011. Persistence of soil organic matter as an ecosystem property. Nature 478, 49–56. https://doi.org/10.1038/nature10386.

Shahbaz, M., Kuzyakov, Y., Sanaullah, M., Heitkamp, F., Zelenev, V., Kumar, A., Blagodatskaya, E., 2017. Microbial decomposition of soil organic matter is mediated by quality and quantity of crop residues: mechanisms and thresholds. Biol. Fertil. Soils 53, 287–301. https://doi.org/10.1007/s00374-016-1174-9.

Sinsabaugh, R.L., Manzoni, S., Moorhead, D.L., Richter, A., 2013. Carbon use efficiency of microbial communities: stoichiometry, methodology and modelling. Ecol. Lett. 16, 930–939. https://doi.org/10.1111/ele.12113.

Su, Z., Shangguan, Z., 2023. Nitrogen addition decreases the soil cumulative priming effect and favours soil net carbon gains in robinia pseudoacacia plantation soil. Geoderma 433, 116444. https://doi.org/10.1016/j.geoderma.2023.116444.

Villarino, S.H., Pinto, P., Jackson, R.B., Piñeiro, G., 2025. Plant rhizodeposition: a key factor for soil organic matter formation in stable fractions. Sci. Adv. 7, eabd3176. https://doi.org/10.1126/sciadv.abd3176.

Wang, C., Kuzyakov, Y., 2024. Rhizosphere engineering for soil carbon sequestration. Trends Plant Sci. 29, 447–468. https://doi.org/10.1016/j.tplants.2023.09.015.

Wang, C., Shi, Z., Li, A., Geng, T., Liu, L., Liu, W., 2024a. Long-term nitrogen input reduces soil bacterial network complexity by shifts in life history strategy in temperate grassland. iMeta. https://doi.org/10.1002/imt2.194.

Wang, Q., Wang, J., Zhang, Z., Li, M., Wang, D., Zhang, P., Li, N., Yin, H., 2024b. Microbial metabolic traits drive the differential contribution of microbial necromass to soil organic carbon between the rhizosphere of absorptive roots and transport roots. Soil Biol. Biochem. 197, 109529. https://doi.org/10.1016/j.soilbio.2024.109529.

Wang, Z., Li, D., Gruda, N.S., Duan, Z., Li, X., 2024c. Fertilizer application rate and nutrient use efficiency in Chinese greenhouse vegetable production. Resour. Conserv. Recycl. 203, 107431. https://doi.org/10.1016/j.resconrec.2024.107431.

Whitaker, J., Ostle, N., Nottingham, A.T., Ccahuana, A., Salinas, N., Bardgett, R.D., Meir, P., McNamara, N.P., 2014. Microbial community composition explains soil respiration responses to changing carbon inputs along an Andes-to-Amazon elevation gradient. J. Ecol. 102, 1058–1071. https://doi.org/10.1111/1365-2745.12247.

Wu, J., Joergensen, R.G., Pommerening, B., Chaussod, R., Brookes, P.C., 1990. Measurement of soil microbial biomass c by fumigation-extraction—an automated procedure. Soil Biol. Biochem. 22, 1167–1169. https://doi.org/10.1016/0038-0717(90)90046-3.

Wu, J., Cheng, X., Luo, Y., Liu, W., Liu, G., 2022. Identifying Carbon-Degrading enzyme activities in association with soil organic carbon accumulation under Land-Use changes. Ecosystems 25, 1219–1233. https://doi.org/10.1007/s10021-021-00711-y.

Xu, X., Zhang, Q., Song, M., Zhang, X., Bi, R., Zhan, L., Dong, Y., Xiong, Z., 2022. Soil organic carbon decomposition responding to warming under nitrogen addition across Chinese vegetable soils. Ecotoxicol. Environ. Saf. 242, 113932. https://doi.org/10.1016/j.ecoenv.2022.113932.

Yang, S., Zhao, X., Wang, Q., Tian, P., 2024. Greater influences of nitrogen addition on priming effect in forest subsoil than topsoil regardless of incubation warming. Sci. Total Environ. 946, 174308. https://doi.org/10.1016/j.scitotenv.2024.174308.

Yang, Y., Xie, H., Mao, Z., Bao, X., He, H., Zhang, X., Liang, C., 2022. Fungi determine increased soil organic carbon more than bacteria through their necromass inputs in conservation tillage croplands. Soil Biol. Biochem. 167, 108587. https://doi.org/10.1016/j.soilbio.2022.108587.

Yin, L., Dijkstra, F.A., Phillips, R.P., Zhu, B., Wang, P., Cheng, W., 2021. Arbuscular mycorrhizal trees cause a higher carbon to nitrogen ratio of soil organic matter decomposition via rhizosphere priming than ectomycorrhizal trees. Soil Biol. Biochem. 157, 108246. https://doi.org/10.1016/j.soilbio.2021.108246.

Zang, H., Blagodatskaya, E., Wang, J., Xu, X., Kuzyakov, Y., 2017. Nitrogen fertilization increases rhizodeposit incorporation into microbial biomass and reduces soil organic matter losses. Biol. Fertil. Soils 53, 419–429. https://doi.org/10.1007/s00374-017-1194-0.

Zhang, S., Xu, Y., Zheng, M., Yang, W., Wang, Y., Liu, S., Zhao, Y., Cha, X., Zhao, F., Han, X., Yang, G., Zhang, C., Ren, C., 2024. Regulation of nutrient addition-induced priming effect by both soil c accessibility and nutrient limitation in afforested ecosystem. Catena 238, 107889. https://doi.org/10.1016/j.catena.2024.107889.

Zhang, Y., Gao, W., Ma, L., Luan, H., Tang, J., Li, R., Li, M., Huang, S., Wang, L., 2023. Long-term partial substitution of chemical fertilizer by organic amendments influences soil microbial functional diversity of phosphorus cycling and improves phosphorus availability in greenhouse vegetable production. Agric. Ecosyst. Environ. 341, 108193. https://doi.org/10.1016/j.agee.2022.108193.

Zheng, Y., Jin, J., Wang, X., Clark, G.J., Tang, C., 2022. Increasing nitrogen availability does not decrease the priming effect on soil organic matter under pulse glucose and single nitrogen addition in woodland topsoil. Soil Biol. Biochem. 172, 108767. https://doi.org/10.1016/j.soilbio.2022.108767.

Zhou, S., Wang, Jieying, Chen, L., Wang, Jun, Zhao, F., 2022. Microbial community structure and functional genes drive soil priming effect following afforestation. Sci. Total Environ. 825, 153925. https://doi.org/10.1016/j.scitotenv.2022.153925.